9638 *Biochemistry* **2010,** *49,* 9638–9648
DOI: 10.1021/bi100651v

BIOCHEMISTRY
including biophysical chemistry & molecular biology
Article

Unique Biogenesis of High-Molecular Mass Multimeric Metalloenzyme Nitrile Hydratase: Intermediates and a Proposed Mechanism for Self-Subunit Swapping Maturation†

Zhemin Zhou,[‡,§,⊥] Yoshiteru Hashimoto,[‡,⊥] Tianwei Cui,[‡,⊥] Yumi Washizawa,[‡] Hiroyuki Mino,[∥] and Michihiko Kobayashi*[,‡]

[‡]*Institute of Applied Biochemistry and Graduate School of Life and Environmental Sciences, The University of Tsukuba, 1-1-1 Tennodai, Tsukuba, Ibaraki 305-8572, Japan,* [§]*Key Laboratory of Industrial Biotechnology* (*Ministry of Education*), *School of Biotechnology, Jiangnan University, 1800 Lihu Avenue, Wuxi, Jiangsu 214122, China, and* [∥]*Division of Material Science* (*Physics*), *Graduate School of Science, Nagoya University, Nagoya 464-8602, Japan*
[⊥]*These authors contributed equally to this work.*

Received April 27, 2010; Revised Manuscript Received October 1, 2010

ABSTRACT: *Rhodococcus rhodochrous* J1 produces high- and low-molecular mass nitrile hydratases (H-NHase and L-NHase, respectively), depending on the inducer. The incorporation of cobalt into L-NHase has been found to depend on the α-subunit exchange between cobalt-free L-NHase (apo-L-NHase) and its cobalt-containing mediator, NhlAE (holo-NhlAE), this novel mode of post-translational maturation having been named self-subunit swapping and NhlE having been recognized as a self-subunit swapping chaperone. We discovered an H-NHase maturation mediator, NhhAG, consisting of NhhG and the α-subunit of H-NHase. The incorporation of cobalt into H-NHase was confirmed to be dependent on self-subunit swapping. For the first time, particles larger than apo-H-NHase were observed during the swapping process via dynamic light scattering measurements, suggesting the formation of intermediate complexes. On the basis of these findings, we initially proposed a possible mechanism for self-subunit swapping. Electron paramagnetic resonance analysis demonstrated that the coordination environment of a cobalt ion in holo-NhhAG is subtly different from that in H-NHase. Cobalt is inserted into cobalt-free NhhAG (apo-NhhAG) but not into apo-H-NHase, suggesting that NhhG functions not only as a self-subunit swapping chaperone but also as a metallochaperone. In addition, α-subunit swapping did not occur between apo-L-NHase and holo-NhhAG or between apo-H-NHase and holo-NhlAE in vitro. These findings revealed that self-subunit swapping is a subunit-specific reaction.

Nitrile hydratase (NHase,[1] EC4.2.1.84) (*1*, *2*), which is composed of α- and *β*-subunits, contains either non-heme iron (*3*, *4*) or non-corrin cobalt ion (*5*−*7*). NHase catalyzes the hydration of a nitrile to the corresponding amide, followed by consecutive reactions: amide → acid → acyl-CoA, catalyzed by amidase (*8*) and acyl-CoA synthetase (*9*, *10*), respectively. *Rhodococcus rhodochrous* J1 (*11*, *12*) produces high- and low-molecular mass NHases (H-NHase and L-NHase, respectively), which exhibit different physicochemical properties and substrate specificities (*1*, *13*). In both H-NHase and L-NHase, cobalt acts as an active center for the production of acrylamide and nicotinamide. Acrylamide is manufactured at the industrial level not only in Japan but also in the United States and France (*14*, *15*). In addition, non-corrin cobalt has been the subject of growing interest not only in bioinorganic chemistry but also in biotechnology, and its availability and remarkable chemical versatility make it an invaluable catalyst in the chemical industry (*16*−*19*).

Metal ions in both Co-NHase and Fe-NHase are located in their α-subunits, which share a characteristic metal-binding motif [CXLC(SO_2H)SC(SOH)] containing two modified cysteine residues: cysteinesulfinic acid (αCys-SO_2H) and cysteinesulfenic acid (αCys-SOH) (*4*, *20*−*24*). The apoenzyme is likely to be nonmodified, judging from the results of the previous studies on NHase (*25*) and a related enzyme, thiocyanate hydrolase (SCNase) (*26*−*28*).

Metalloproteins have been characterized intensively for decades, yet only recently have investigators focused on the mechanisms of biological metallocenter assembly. Several general mechanisms of metallocenter biosynthesis have been reviewed (*29*), as follows: (i) reversible metal ion binding, (ii) metallochaperone delivery of a metal ion or cofactor, (iii) post-translational modification creating a metal-binding site, (iv) synergistic binding of a metal with another

†This work was supported in part by a Grant-in-Aid for Scientific Research from the Ministry of Education, Culture, Sports, Science, and Technology (MEXT).

*To whom correspondence should be addressed: Institute of Applied Biochemistry and Graduate School of Life and Environmental Sciences, The University of Tsukuba, 1-1-1 Tennodai, Tsukuba, Ibaraki 305-8572, Japan. Fax: +81-29-853-4605 (Institute).

[1]Abbreviations: NHase, nitrile hydratase; H-NHase, high-molecular mass nitrile hydratase; L-NHase, low-molecular mass nitrile hydratase; SCNase, thiocyanate hydrolase; NhhAG, H-NHase maturation mediator complex (αg_2); NhlAE, L-NHase maturation mediator complex (αe_2); pHJK19$_{(\Delta G)}$, plasmid pHJK19 without the *nhhG* gene; H-NHase$_{(+G)}$, H-NHase expressed from pHJK19; H-NHase$_{(\Delta G)}$, H-NHase expressed from pHJK19$_{(\Delta G)}$; R-H-NHase, reconstituted H-NHase derived from a mixture of holo-NhhAG and apo-H-NHase; DLS, dynamic light scattering; R-apo-H-NHase$_{(NhlAE)}$, resultant H-NHase derived from a mixture of holo-NhlAE and apo-H-NHase; R-apo-L-NHase$_{(NhhAG)}$, resultant L-NHase derived from mixture of holo-NhhAG and apo-L-NHase.

 Published on Web 10/01/2010 © 2010 American Chemical Society

component, (v) synthesis of metal-containing cofactors, (vi) metal incorporation coupled with electron transfer, (vii) requirement for an apoprotein-specific molecular chaperone, etc. In all cases, the components of the apoprotein remain in the final holoprotein. Very recently, we discovered a novel mode of post-translational maturation for L-NHase (encoded by genes *nhlBA* and consisting of $\alpha_2\beta_2$): it depends on swapping of the unmodified and metal-free α-subunit in the L-NHase complex with the oxidized and cobalt-containing α-subunit from the L-NHase mediator complex, NhlAE (encoded by genes *nhlAE* and consisting of αe_2) (Figure S1 of the Supporting Information) (*30*). This post-translational maturation process is different from general mechanisms of metallocenter biosynthesis known so far, and we thus named it self-subunit swapping (*30*). Compared with activators acting as metallochaperones in ferric NHases (*31*) from *Rhodococcus* sp. N-771 (*32*), *Pseudomonas putida* 5B (*33*), *Rhodococcus* sp. N-774 (*34*), etc., NhlE acts as a self-subunit swapping chaperone, exhibiting novel behavior for a protein in a protein complex (*30*). Furthermore, oxidation of the metal ligand cysteine residues and insertion of cobalt into the α-subunit are conducted in an NhlE-dependent manner (*35*). Cysteine modification has been demonstrated to exist in cobalt-containing NhlAE (holo-αe_2), but not in cobalt-free NhlAE (apo-αe_2), and cysteine oxidation plays an essential role in self-subunit swapping maturation (*30*).

Self-subunit swapping represents a new concept in the history of protein complex research. To date, only L-NHase has been reported to mature through self-subunit swapping. On the basis of the several similar features (i.e., enzyme properties, gene organizations, etc.) of various Co-NHases and a NHase family enzyme, SCNase, we expected that self-subunit swapping would occur in these enzymes and confirmed the self-subunit swapping maturation of H-NHase. Here, we provide evidence of the generality of self-subunit swapping maturation for multimeric NHases and reveal that self-subunit swapping is a subunit-specific reaction.

EXPERIMENTAL PROCEDURES

Strains and Plasmids. *R. rhodochrous* ATCC12674 was used as the host for vector plasmids pHJK19 (*13*), pHJK19$_{(\Delta G)}$, and pHJK19$_{(\alpha\text{-V5L})}$ (Figure S2 of the Supporting Information), which were used for expression of H-NHase and its mutants. *Escherichia coli* DH10B was the host used for plasmid pHJK19$_{(\Delta G)}$ and pHJK19$_{(\alpha\text{-V5L})}$ construction. *E. coli* JM109 was the host for plasmid pHJK19 methylation. *Rhodococcus fascians* DSM43985 was used as the host for vector plasmid pREIT19, which was used for expression of *nhlBAE*, *nhhA*−*nhlE*, and *nhlAE* (Figure S2 of the Supporting Information), as described previously (*30*).

Construction of Plasmids. Inverse polymerase chain reaction (PCR) (*36*) was performed for pHJK19$_{(\Delta G)}$ and pHJK19$_{(\alpha\text{-V5L})}$ construction. PCR was performed with primers BA-S and BA-AS (Table S1 of the Supporting Information), using methylated pHJK19 as the template, to produce the full-length linear pHJK19$_{(\Delta G)}$. The PCR product was digested with DpnI to degrade the template plasmid and then ligated to circular pHJK19$_{(\Delta G)}$ with Ligation High (Toyobo Co., Ltd., Osaka, Japan) and used to transform *E. coli* DH10B. After sequencing, a clone with the sequence of pHJK19$_{(\Delta G)}$ was chosen and transformed into *R. rhodochrous* ATCC12674. Plasmid pHJK19$_{(\alpha\text{-V5L})}$ was constructed in the same manner as pHJK19$_{(\Delta G)}$, except that primers A-V5L-S and A-V5L-AS (Table S1 of the Supporting Information) were used, and then was transformed into *R. rhodochrous* ATCC12674.

An overlap extension PCR protocol (*37*) was used for plasmid pREIT-*nhhA-nhlE* construction. Two PCRs, with the primer pair A*G-up and A*-E-AS (Table S1 of the Supporting Information) and plasmid pHJK19 as the template and the primer pair A*-E-S and E-down (Table S1 of the Supporting Information) and plasmid pREIT-*nhlAE* as the template, were performed for the first round. Equimolar amounts of the first-round products were mixed as the template for the next PCR. The second round of PCR was performed with the primer pair A*G-up and E-down. The PCR products were digested with XbaI and SacI, ligated into pUC19, and then sequenced. The clones with the correct sequences were chosen, digested with XbaI and SacI, and then ligated into pREIT19 to construct pREIT-*nhhA-nhlE*, the resultant plasmids being transformed into *R. fascians* DSM43985.

Culture Conditions. Electroporation was performed for the transformation of *R. rhodochrous* ATCC12674, as described previously (*13*). The *R. rhodochrous* ATCC12674 transformants carrying pHJK19, pHJK19$_{(\Delta G)}$, and pHJK19$_{(\alpha\text{-V5L})}$ were each grown at 28 °C for 48 h in MYP medium (*38*) containing $CoCl_2 \cdot 6H_2O$ (0.05 g/L) and neomycin (50 μg/mL), as described previously (*13*). *R. fascians* DSM43985 cells carrying plasmid pREIT-*nhlBAE*, pREIT-*nhlAE*, or pREIT-*nhhA-nhlE* were incubated separately under the conditions described previously (*30*) for expression of L-NHase, NhlAE, or the NhhA−NhlE hybrid mediator complex, respectively.

Purification of Enzymes. All purification steps were performed at 0−4 °C. Ten millimolar potassium phosphate buffer (KPB, pH 7.5) was used in all purification steps. All procedures except ammonium sulfate precipitation were conducted with an AKTA purifier (GE Healthcare UK Ltd.).

Cell extract preparation was performed as described previously (*13*). Centrifugation was conducted for 20 min at 18000*g*. H-NHase was partially purified by ammonium sulfate fractionation (40−65%), followed by dialysis against the same buffer. The dialyzed solution was applied to a DEAE-Sephacel column (3 × 5 mL) (GE Healthcare UK Ltd.) equilibrated with the same buffer. We eluted the protein from the column with 1 L of the same buffer by increasing the concentration of KCl linearly from 0 to 0.5 M. The resultant partially purified enzyme was pooled, and then ammonium sulfate was added to give 70% saturation. After centrifugation of the suspension, the precipitate was dissolved in 0.2 M KCl-containing 10 mM KPB (pH 7.5), followed by application to a Hiload 16/60 Superdex 200 pg column (GE Healthcare UK Ltd.) equilibrated with the 0.2 M KCl-containing buffer. The enzyme that eluted from the Hiload 16/60 Superdex 200 pg column was precipitated with ammonium sulfate (70% saturation), followed by dialysis against the same buffer. The dialyzed solution was applied to a Resource Q column (6 mL) (GE Healthcare UK Ltd.) equilibrated with the same buffer. We eluted proteins from the column with 1 L of the same buffer by increasing the concentration of KCl linearly from 0 to 0.5 M. NhhAG was purified in the same manner as H-NHase. The fractions containing the proteins during the purification steps were revealed by sodium dodecyl sulfate−polyacrylamide gel electrophoresis (SDS−PAGE), and sequence analysis of N-terminal amino acids was the last step. L-NHase and NhlAE were purified as described previously (*30*). Hiload 16/60 Superdex 200 pg was used to purify the reconstituted enzymes from mixtures as described above.

Enzyme Assays. H-NHase activity was assayed in a reaction mixture (0.5 mL) comprising 10 mM KPB (pH 7.5), 500 mM 3-cyanopyridine, and an appropriate amount of the enzyme.

The reaction was conducted at 20 °C for 20 min and stopped by the addition of 4.5 mL of acetonitrile. The amount of nicotinamide formed in the reaction mixture was determined by HPLC with a Shimadzu (Kyoto, Japan) LC-10A system equipped with a Cosmosil $5C_{18}$-AR-II column [reversed phase, 4.6 mm × 150 mm (Nacalai Tesque, Kyoto, Japan)] and the UV spectrophotometric detector (SPD-M10A) of the original system. The following solvent system was used: 5 mM KH_2PO_4/H_3PO_4 buffer (pH 2.9) and acetonitrile (2:1, v/v), at a flow rate of 1.0 mL/min. A wavelength of 215 nm was used for monitoring. One unit of H-NHase activity was defined as the amount of enzyme that catalyzed the release of 1 μmol of nicotinamide per minute at 20 °C. L-NHase activity was assayed as described previously (*30*).

Protein Molecular Mass Determination. Superose 6 HR 10/30 and Superose 12 HR 10/30 (GE Healthcare UK Ltd.) columns and 0.2 M KCl-containing 10 mM KPB (pH 7.5) were used for estimation of the molecular masses of the purified H-NHases and NhhAG, respectively. This step was conducted with an AKTA purifier (GE Healthcare UK Ltd.) at 0−4 °C, with a flow rate of 0.5 mL/min.

Electron Paramagnetic Resonance (EPR) Spectroscopy. Reduced proteins were prepared by the addition of a 30-fold excess of reduced methyl viologen, prepared by the addition of sodium dithionite to methyl viologen in 10 mM KPB (pH 7.5), to a sample of enzyme (final concentration of 5 mg/mL) prepared under argon. The reduction of each sample was confirmed by the color of methyl viologen after the addition of sodium dithionite. The sample was frozen after 15 min on ice and stored in liquid nitrogen. EPR spectra were recorded using a Bruker ESP-300E X-band spectrometer (Bruker Biospin) equipped with a liquid helium flow cryostat and a temperature control system (CF935, Oxford Instruments, Oxford, U.K.). The conditions were as follows: microwave frequency, 9.52 GHz; modulation amplitude, 20 G; microwave power, 3.2 mW; temperature, 20 K; and scan rate, 50 G/s. Simulation of the EPR spectrum was performed using Easyspin version 3.1.1 (*39*).

Analytical Methods. Circular dichroism (CD) measurements were taken with a Jasco spectropolarimeter (model J-720W, Japan Spectroscopic Co., Tokyo, Japan), equipped with a thermal incubation system, at 20 °C with a 1 mm light path cell. The CD spectra were recorded at a protein concentration of 0.2 mg/mL in 10 mM KPB (pH 7.5) in the far-UV region (200−260 nm) and at a protein concentration of 1 mg/mL in 10 mM KPB (pH 7.5) in the near-UV−vis region (300−750 nm). UV−vis spectra were recorded with a Shimadzu UV-1700 spectrophotometer at room temperature. Enzymes were dialyzed against 10 mM KPB (pH 7.5) and then prepared at 5.0 mg/mL. The NH_2-terminal amino acid sequences were determined with samples electroblotted onto polyvinylidene difluoride membranes after SDS−PAGE using a Procise protein sequencer (Applied Biosystems).

Size Measurement. Apo-NHase (final concentration of 0.05 mg/mL), holo-NHase (final concentration of 0.05 mg/mL), and a mixture of apo-NHase and holo-NhhAG (final concentrations of 0.05 and 0.5 mg/mL, respectively) in 10 mM KPB (pH 7.5) were used to determine their sizes by means of dynamic light scattering (DLS) on a Zetasizer Nano ZS (Malvern Instruments, Ltd.) equipped with a 4 mW He−Ne ion laser (λ = 633 nm). The DLS measurements were taken at 20 °C at a detection angle of 173°. The obtained correlation functions were analyzed by the cumulant method to determine the hydrodynamic diameters.

Cobalt Ion Determination. Proteins were dialyzed against 1 mM KPB (pH 7.5) and then prepared at 0.5 mg/mL. After dialysis, the enzymes were detected with a Nippon Jarrell-Ash (Kyoto, Japan) ICAP-575 emission spectrometer under the following conditions: wavelength, 238.89 nm; integral time, 3 s; and voltage, 850 mV.

RESULTS

Comparison of a Self-Subunit Swapping Chaperone with Other Co-NHase-Related Proteins. A search using the BLAST program revealed that the self-subunit swapping chaperone NhlE exhibits significant sequence similarity to various small proteins, the genes of which are located just downstream of the structural genes of other NHases and putative NHases (Table S2 of the Supporting Information). All of these NHases have the same features as L-NHase. (i) The putative metal-binding motif in the α-subunit is the same as that of Co-NHase (-CTLCSC-, conserved in all reported Co-NHases) but not that of Fe-NHase (-CSLCSC-, conserved in all reported Fe-NHases), suggesting that all of them are Co-NHases (Figure S3 of the Supporting Information). (ii) The structural genes for the α- and β-subunits are in the order β and α (Figure S3 of the Supporting Information). (iii) The molecular masses of the small proteins are less than 17 kDa (Table S2 of the Supporting Information). (iv) The small proteins exhibit meaningful sequence similarity to the NHase β-subunits. (v) All of these small proteins lack known metal-binding motifs. Among these NHases, H-NHase in *R. rhodoccocus* J1 and NHase in *Bacillus pallidus* RAPc8 have been well characterized (*13*, *40*). H-NHase has been successfully expressed using *R. rhodoccocus* ATCC12674 as a host carrying plasmid pJHK19, which contains both the H-NHase genes (*nhhBA*) and the small gene (*nhhG*) just downstream of the H-NHase α-subunit gene (*nhhA*) (*13*). In *B. pallidus* RAPc8, the small gene, *p14k*, just downstream of the α-subunit gene of NHase has been found to be necessary for functional expression of this NHase (*40*). These findings permit us to speculate that self-subunit swapping maturation also occurs in these other Co-NHases. Therefore, the following experiments were conducted to determine whether self-subunit swapping occurs during the post-translational maturation of H-NHase.

Necessity of nhhG for Functional H-NHase Expression. Plasmid pJHK19 (Figure S2 of the Supporting Information) used for H-NHase expression carries the H-NHase genes (*nhhBA*) and five other ORFs (*nhhC*, *nhhD*, *nhhE*, *nhhF*, and *nhhG*) (*13*). Of these ORFs, *nhhC* and *nhhD* are indispensable for the intracellular formation of an active recombinant H-NHase in *R. rhodoccocus* ATCC12674, whereas *nhhE* and *nhhF* have been found to have no influence on the expression of the H-NHase gene (*13*). However, the participation of *nhhG* in the H-NHase gene expression remains to be confirmed. We here constructed a plasmid, $pHJK19_{(\Delta G)}$ (Figure S2 of the Supporting Information), that contains *nhhC*, *nhhD*, *nhhE*, *nhhF*, and H-NHase structural genes *nhhBA* but lacks *nhhG*. *R. rhodochrous* ATCC12674 cells harboring $pHJK19_{(\Delta G)}$ were used to express H-NHase under the same conditions that were used for *R. rhodochrous* ATCC12674 harboring pHJK19. The bands of the α- and β-subunits of H-NHase were obvious on sodium dodecyl sulfate−polyacrylamide gel electrophoresis (SDS−PAGE) (Figure 1A), while the activity in cell-free extracts of the *Rhodococcus* transformant was very low (2.4 ± 1.5 units/mg). On the other hand, the amount of H-NHase expressed using *R. rhodochrous* ATCC12674 cells harboring pHJK19 was similar to that of $pHJK19_{(\Delta G)}$, and the H-NHase activity (121 ± 10 units/mg) in cell-free extracts was much higher than that of $pHJK19_{(\Delta G)}$.

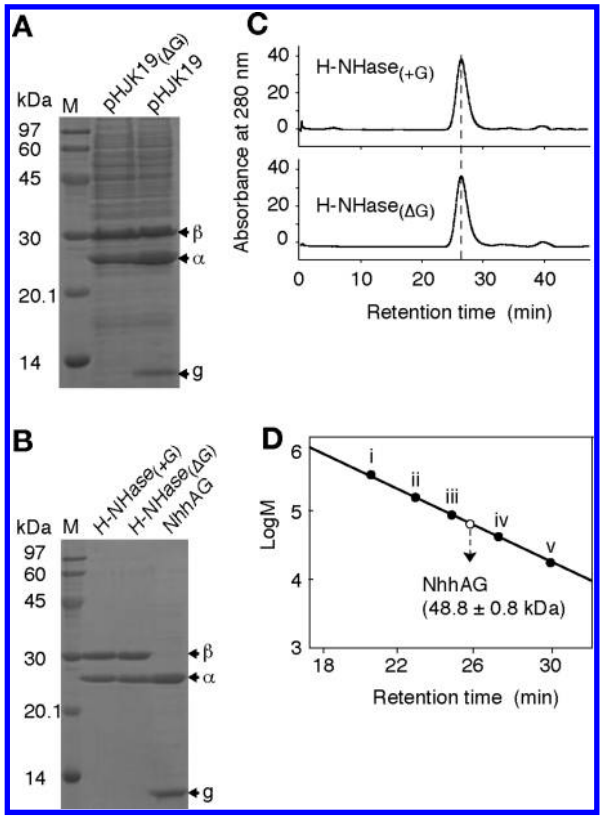

FIGURE 1: Expression and purification of H-NHase and NhhAG. SDS−PAGE of a cell-free extract of each *R. rhodochrous* ATCC12674 transformant (A) and the purified H-NHases and NhhAG (B). (C) Gel filtration profiles from a Superose 6 HR 10/30 column of the purified H-NHases. (D) Determination of the molecular masses and structures of NhhAG on a Superose 12 HR 10/30 column. *nhhA* and *nhhG* [DDBJ accession numbers BAA11044 (*nhhA*) and BBA11045 (*nhhG*)] should encode proteins of 203 amino acids (22.8 kDa) and 104 amino acids (11.7 kDa), respectively. The following marker proteins were used for gel filtration: (i) glutamate dehydrogenase (yeast) (290 kDa), (ii) lactate dehydrogenase (pig heart) (142 kDa), (iii) enolase (yeast) (67 kDa), (iv) myokinase (yeast) (32 kDa), and (v) cytochrome *c* (horse heart) (12.4 kDa). The molecular mass determined is shown as a white circle. The values obtained on gel filtration shown represent the means ± the standard deviation for three independent experiments.

To determine the differences between the H-NHases expressed from pHJK19 and pHJK19$_{(\Delta G)}$, we completely purified and characterized the two enzymes (Figure 1B). Hereafter, we refer to the H-NHases expressed from pHJK19 and pHJK19$_{(\Delta G)}$ as H-NHase$_{(+G)}$ and H-NHase$_{(\Delta G)}$, respectively. As a result, H-NHase$_{(+G)}$ was found to be a multimer of $\alpha\beta$ heterodimers (approximately 500 kDa) identical in size to that purified from *R. rhodochrous* J1 (*41*); H-NHase$_{(\Delta G)}$ has the same molecular mass as H-NHase$_{(+G)}$ (Figure 1C). Compared with the specific activity of 298 ± 8 units/mg exhibited by H-NHase$_{(+G)}$, H-NHase$_{(\Delta G)}$ exhibited a very low activity (6.8 ± 1.2 units/mg) (Table 1). The cobalt content [which is essential for the activity (*1*, *19*)] of H-NHase$_{(+G)}$ was found to be 0.90 ± 0.04 mol/mol of $\alpha\beta$, whereas that of H-NHase$_{(\Delta G)}$ was low (0.33 ± 0.02 mol/mol of $\alpha\beta$) (Table 1). Although H-NHase$_{(+G)}$ and H-NHase$_{(\Delta G)}$ exhibited similar far-UV CD spectra (Figure 2A), the near-UV−vis CD spectrum and the UV−vis spectrum of H-NHase$_{(+G)}$ were not similar to those of H-NHase$_{(\Delta G)}$ (Figure 2B,C). The band at 340 nm in the near-UV−vis CD spectrum and the absorption in the 300−350 nm region of H-NHase$_{(+G)}$ have been reported to be derived from the S → Co^{3+} charge transfer

Table 1: Characterization of the Purified H-NHases and NhhAG[a]

protein (plasmid)	cobalt content (mol of ions/mol of protein)	specific activity (units/mg)
H-NHase$_{(+G)}$ (pHJK19)	0.90 ± 0.04/$\alpha\beta$	298 ± 8
H-NHase$_{(\Delta G)}$ [pHJK19$_{(\Delta G)}$]	0.33 ± 0.02/$\alpha\beta$	6.8 ± 1.2
apo-H-NHase (pHJK19)	0.04 ± 0.01/$\alpha\beta$	2.4 ± 0.5
NhhAG (pHJK19)	0.84 ± 0.04/αg_2	0

[a]The plasmids used for the preparation of H-NHase and NhhAG are shown in parentheses following each protein. The values represent the means ± the standard deviation for at least three independent experiments.

character (*7*, *30*, *42*). These findings demonstrate that H-NHase expressed from pHJK19$_{(\Delta G)}$ is a cobalt-deficient H-NHase, in contrast to cobalt-containing H-NHase [holo-H-NHase, i.e., H-NHase$_{(+G)}$] expressed from pHJK19, and that *nhhG* is responsible for functional H-NHase expression. We purified a cobalt-free H-NHase (apo-H-NHase) (Table 1) expressed from pHJK19 (from a culture in the absence of cobalt). Apo-H-NHase exhibited no extra shoulder in the 300−350 nm region in the near-UV−vis CD and UV−vis spectra (Figure 2B,C). Apo-H-NHase exhibited a very low activity (2.4 ± 0.5 units/mg), and its cobalt content was very low (0.04 ± 0.01 mol/mol of $\alpha\beta$) compared with that in the case of H-NHase$_{(\Delta G)}$. Very recently, Odaka and his co-workers reported that the Cys133 residue of the γ-subunit of purified SCNase was modified to Cys-SO(H) during storage, and the Cys133 residue was further oxidized to Cys-SO_2^- during storage under aerobic conditions (*43*). These findings raise the possibility that the Cys107 residue of the α-subunit of H-NHase (corresponding to Cys133 of the SCNase) is likely oxidized, and incorrect Cys oxidation may occur during cultivation of the *R. rhodochrous* ATCC12674 transformant carrying pHJK19$_{(\Delta G)}$ in the medium containing cobalt, yielding H-NHase$_{(\Delta G)}$ with an $\alpha\beta$ cobalt content of 0.33 ± 0.02 mol/mol and a very low activity. Thus, apo-H-NHase was used for the following experiments as an apoenzyme for H-NHase instead of H-NHase$_{(\Delta G)}$.

Cobalt-Containing H-NHase Mediator NhhAG. To clarify the role of *nhhG* in the post-translational activation of H-NHase, we purified the gene product (NhhG) from the transformant harboring pHJK19. As a result, NhhG was confirmed to form a complex (i.e., NhhAG) with the α-subunit of H-NHase (Figure 1B); the molecular mass of the recombinant NhhAG was determined to be 48.8 ± 0.8 kDa (Figure 1D) by gel filtration analysis. Because the calculated molecular masses of the α-subunit and NhhG are 22.8 and 11.7 kDa, respectively, NhhAG consists of a heterotrimer, αg_2 (46.2 kDa). The purified αg_2 exhibited no H-NHase activity, while it contained a cobalt ion (0.84 ± 0.04 mol/mol of αg_2) (Table 1). The cobalt-containing αg_2 is termed holo-NhhAG. The near-UV−vis CD spectrum of holo-NhhAG (Figure 2E) exhibited a band at 346 nm. The UV−vis spectrum of holo-NhhAG also exhibited an extra shoulder in the 300−350 nm region (Figure 2F).

NhhAG is very similar to the mediator of L-NHase, NhlAE, which is a heterotrimer complex (αe_2) consisting of the cobalt-containing α-subunit of L-NHase and NhlE (which is denoted as e) (*30*). NhlAE has been reported to incorporate cobalt ions into apo-L-NHase during the post-translational maturation of L-NHase, resulting in the formation of holo-L-NHase (*30*). To elucidate the role of NhhAG in the formation of active H-NHase, we conducted the following experiments. The purified apo-H-NHase (final concentration, 0.01 mg/mL) was mixed with the purified holo-NhhAG (final concentration, 0.1 mg/mL), followed by incubation in 10 mM KPB (pH 7.5) at 28 °C.

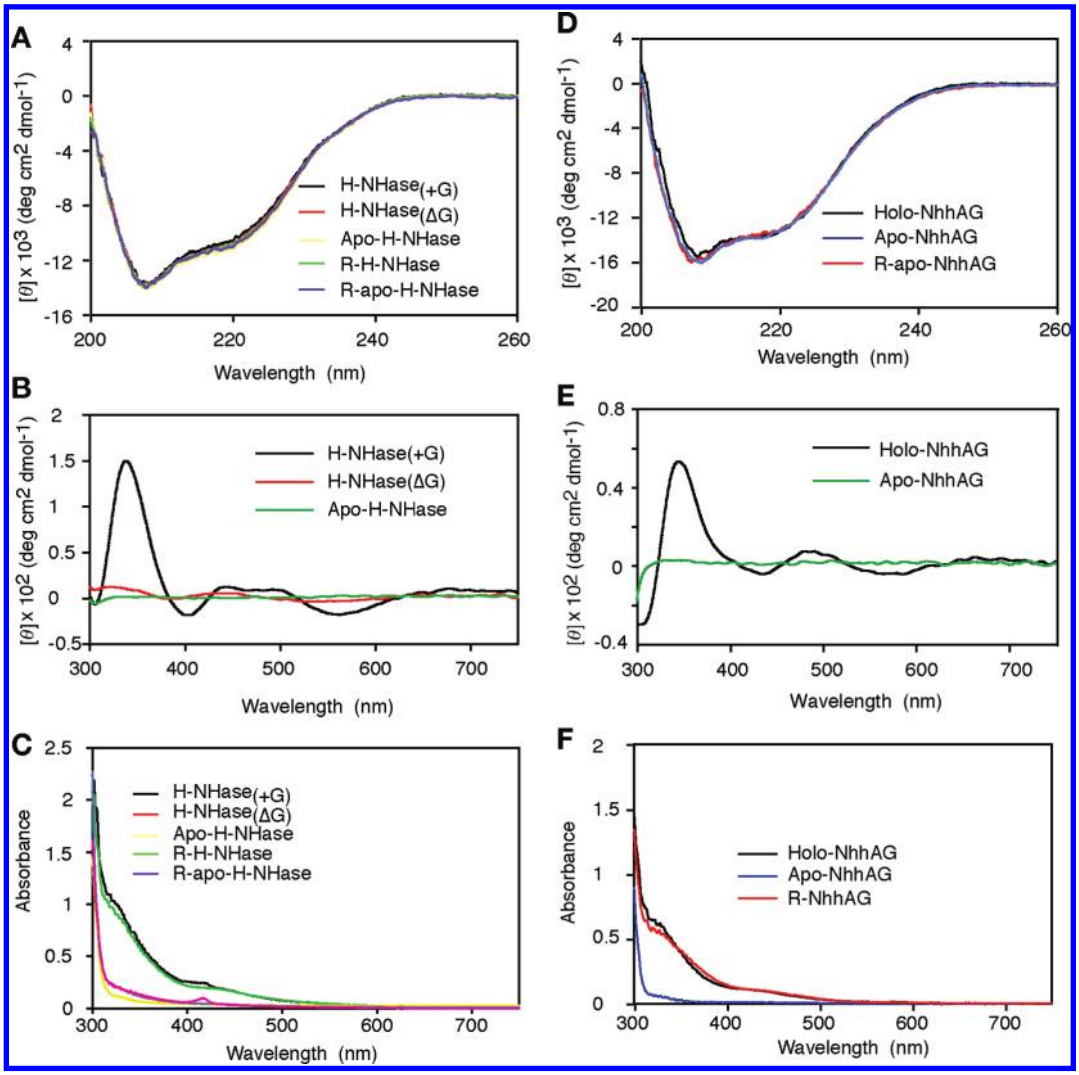

FIGURE 2: Far-UV CD (A and D), near-UV−vis CD (B and E), and UV−vis absorption (C and F) spectra of the purified H-NHases, reconstituted H-NHases, purified NhhAGs, and reconstituted apo-NhhAG. The CD spectra were recorded at a protein concentration of 0.2 mg/mL in 10 mM KPB (pH 7.5) in the far-UV region (200−260 nm) and at a protein concentration of 1 mg/mL in 10 mM KPB (pH 7.5) in the near-UV−vis region (300−750 nm). UV−vis spectra were recorded with a Shimadzu UV-1700 spectrophotometer at room temperature at a protein concentration of 5 mg/mL in 10 mM KPB (pH 7.5).

H-NHase activity in the mixture was found to increase as the incubation time increased (Figure 3A). As the holo-NhhAG concentration increased, the activation rate became higher (Figure 3A). From a mixture of apo-H-NHase and a 10-fold excess of holo-NhhAG, we then purified the reconstituted H-NHase (R-H-NHase), finding that its activity (275 ± 9 units/mg) and cobalt content (0.91 ± 0.03 mol/mol of $\alpha\beta$) (Table 2) were similar to those of holo-H-NHase [H-NHase$_{(+G)}$] (Table 1). Through far-UV CD and UV−vis absorbance spectral analyses, we conducted a detailed comparison of each property of holo-H-NHase, apo-H-NHase, and R-H-NHase. Although R-H-NHase, holo-H-NHase, and apo-H-NHase exhibited similar far-UV CD spectra (Figure 2A), the UV−vis spectrum of R-H-NHase was similar to that of holo-H-NHase, but not to that of apo-H-NHase (Figure 2C). Like holo-H-NHase, R-H-NHase also exhibited an extra shoulder in the 300−350 nm region. These results suggested that the Co ligand environment of R-H-NHase is the same as that of holo-H-NHase. Together with the inclusion of cobalt in R-H-NHase, these phenomena thus demonstrate that NhhAG participates in the post-translational maturation of H-NHase.

Self-Subunit Swapping in H-NHase. Site-directed mutagenesis and N-terminal amino acid sequence analysis were conducted to confirm the source of the α-subunit in the reconstituted H-NHase. We designed a mutant gene [*nhhCDEFBA*$_{(\alpha\text{-V5L})}$*G*] in which Val5 in the α-subunit was substituted with Leu, constructed pHJK19$_{(\alpha\text{-V5L})}$ (Figure S2 of the Supporting Information), and then purified the mutant apo-H-NHase [apo-H-NHase$_{(\alpha V5L)}$] (from a culture in the absence of cobalt). No significant differences in the specific activities of the purified enzymes were observed between apo-H-NHase$_{(\alpha V5L)}$ and apo-H-NHase (Table 2). We mixed apo-H-NHase$_{(\alpha V5L)}$ with holo-NhhAG, confirmed the post-translational activation of H-NHase in vitro, and then purified the reconstituted H-NHase [R-H-NHase$_{(\alpha V5L)}$] from the mixture. On N-terminal amino acid sequence analysis of the α-subunit of the purified R-H-NHase$_{(\alpha V5L)}$, position 5 of the α-subunit was shown to be Val (Table 2), demonstrating that the apo α-subunit of apo-H-NHase$_{(\alpha V5L)}$ was replaced by the holo α-subunit of holo-NhhAG. Next, we mixed apo-H-NHase$_{(\alpha V5L)}$ with holo-NhhAG, took samples at various intervals, and measured the H-NHase activity, concomitantly purifying the reconstituted H-NHase [R-H-NHase$_{(\alpha V5L)}$] from the mixture. Then, N-terminal amino acid sequence analysis of the α-subunit of the purified R-H-NHase$_{(\alpha V5L)}$ was conducted, and the amount of Val or Leu at position 5 of the α-subunit was determined. As a result, significant correlation was

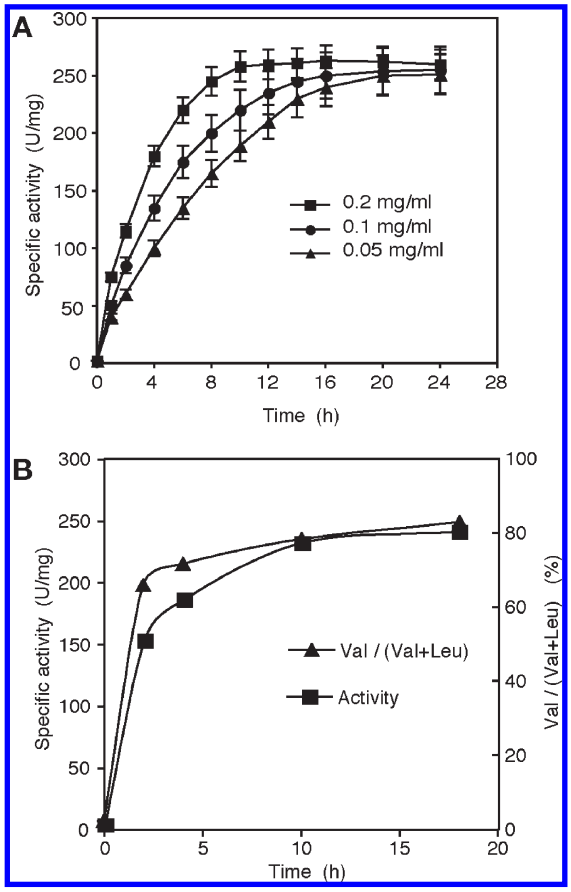

FIGURE 3: Post-translational activation of apo-H-NHase by holo-NhhAG (A) and correlation between the rate of enzyme activation and the rate of self-subunit swapping (B). (A) Apo-H-NHase (final concentration, 0.01 mg/mL) was incubated with purified holo-NhhAG in 10 mM KPB (pH 7.5) at 28 °C. The holo-NhhAG concentration used in the mixture was 0.2, 0.1, or 0.05 mg/mL (final concentration). Samples were removed at the indicated times and then assayed for H-NHase activity. The values represent the means ± the standard deviation for at least four independent experiments. (B) Apo-H-NHase$_{(\alpha V5L)}$ (final concentration, 0.01 mg/mL) was incubated with purified holo-NhhAG (final concentration, 0.1 mg/mL) in 10 mM KPB (pH 7.5) at 28 °C. Samples were removed at the indicated times and then assayed for H-NHase activity. Concomitantly, the reconstituted H-NHase [R-H-NHase$_{(\alpha V5L)}$] was purified from the mixture at each time. The amount of Val or Leu at position 5 of the α-subunit of the R-H-NHase$_{(\alpha V5L)}$ was determined by N-terminal amino acid sequence analysis, and the ratio [Val/(Val + Leu)] in the α-subunit of each purified R-H-NHase$_{(\alpha V5L)}$ was calculated.

Table 2: Characterization of the Purified Apo-H-NHases and the Purified Resultant (R-)H-NHases after Being Mixed with Holo-NhhAG in Vitro[a]

protein	cobalt content (mol of ions/mol of αβ protein)	specific activity (units/mg)	N-terminal sequence of the α-subunit
apo-H-NHase	0.04 ± 0.01	2.4 ± 0.5	^{2}SEH**V**NKY^{8}
R-H-NHase	0.91 ± 0.03	275 ± 9	not tested
apo-H-NHase$_{(\alpha\text{-V5L})}$	0.04 ± 0.01	2.8 ± 0.8	^{2}SEH**L**NKY^{8}
R-H-NHase$_{(\alpha\text{-V5L})}$	0.90 ± 0.05	270 ± 8	^{2}SEH**V**NKY^{8}

[a]The fifth N-terminal amino acid of each α-subunit is shown in bold. Values represent the means ± the standard deviation for at least three independent experiments.

found between the specific activity (as a function of time) and the ratio [Val/(Val + Leu)] in the α-subunit of the purified R-H-NHase$_{(\alpha V5L)}$ (as a function of time) (Figure 3B), demonstrating that the rate of post-translational enzyme activation is almost the same as the rate of self-subunit swapping. These findings revealed that the incorporation of cobalt into apo-H-NHase from holo-NhhAG depended on self-subunit swapping, resulting in the formation of holo-H-NHase and apo-NhhAG, and that NhhG acted as a self-subunit swapping chaperone like the NhlE for L-NHase.

Detection of Large-Sized Complexes during Self-Subunit Swapping in H-NHase. Dynamic light scattering (DLS) experiments were performed, for the first time, to estimate the hydrodynamic diameters and state of the proteins in solution. DLS analyses of apo-H-NHase (final concentration, 0.05 mg/mL) and holo-NhhAG (final concentration, 0.5 mg/mL) exhibited unimodal particle-size distributions with intensity-average hydrodynamic diameters of 14.7 and 6.6 nm, respectively (Figure 4A,B). No change in size was observed in 45 min for apo-H-NHase or holo-NhhAG. When apo-H-NHase (final concentration, 0.05 mg/mL) was mixed with holo-NhhAG (final concentration, 0.5 mg/mL) for self-subunit swapping to occur, two peaks were observed at the following positions: 7.6 and 30.7 nm (Figure 4C). The sizes were monitored through DLS measurement for 45 min after apo-H-NHase and holo-NhhAG had been mixed (Figure 4C,D). Figure 4D shows that the larger-sized particles (than apo-H-NHase) varied in size, with a broad size distribution (hydrodynamic diameters of 21.3−32.0 nm), whereas size variation was hardly observed for the smaller-sized ones. DLS analyses of both holo-H-NHase (final concentration, 0.05 mg/mL) and apo-NhhAG (final concentration, 0.5 mg/mL), which were formed through self-subunit swapping, gave results that were the same as those of apo-H-NHase and holo-NhhAG, respectively (Figure S4A,B of the Supporting Information). These findings suggested that the larger-sized particles observed during self-subunit swapping for H-NHase are intermediate complexes, consisting of apo-H-NHase and holo-NhhAG(s). Considering the size distribution of the larger-sized particles, various kinds of intermediate complexes (i.e., a holo-NhhAG-bound apo-H-NHase, apo-H-NHase bound to two holo-NhhAGs, apo-H-NHase bound to three holo-NhhAGs, and apo-H-NHase bound to some holo-NhhAGs) would exist during the self-subunit swapping process. Moreover, we found that apo-H-NHase and holo-NhhAG combine within 3 min to form large-sized complexes (Figure 4C,D). These findings suggested that the formation of various intermediate complexes is a very rapid process, while α-subunit exchange between apo-H-NHase and holo-NhhAG during self-subunit swapping maturation is a slow process (Figure 3B).

Subtle Difference in the Coordination Environments of the Cobalt Ions between Holo-H-NHase and Holo-NhhAG. The cobalt ion in Co-NHase exists as a low-spin Co^{3+} in a tetragonally distorted octahedral ligand field (*1*, *7*). The assignment of the cobalt ion to low-spin Co^{3+} in H-NHase, NHase of *Pseudomonas putida* NRRL-8668, and SCNase (a Co-NHase family enzyme) has been indirectly supported by EPR data (*7*, *28*, *44*). We here measured EPR spectra of holo-H-NHase, holo-NhhAG, and R-H-NHase (Figure 5). The native holo-H-NHase, holo-NhhAG, and R-H-NHase were EPR-silent (Figure 5A,C,E), as expected for low-spin Co^{3+}. When they were reduced with sodium dithionite and methyl viologen, holo-H-NHase and R-H-NHase exhibited spectra characteristic of low-spin Co^{2+} (Figure 5B,F; $g_{\perp} = 2.185$, $g_{\parallel} = 2.000$, $A^{Co}_{\perp} = 48.6$ G, and $A^{Co}_{\parallel} = 100$ G). These parameters were obtained by computer simulation, as shown in Figure 5G. The main components of the spectrum were reproduced by assuming axial symmetry. The small satellite lines between 3500 and 3750 G were

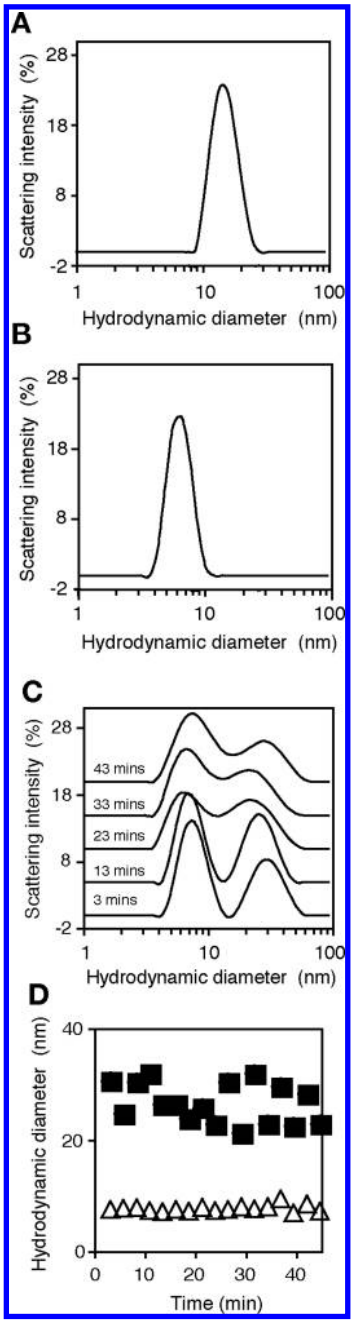

FIGURE 4: Dynamic light scattering (DLS) analyses of apo-H-NHase, holo-NhhAG, and a mixture of apo-H-NHase and holo-NhhAG. Particle-size distributions presented as the light scattering intensity in relation to the hydrodynamic diameter of apo-H-NHase at 3 min (A), holo-NhhAG at 3 min (B), and a mixture of apo-H-NHase and holo-NhhAG at 3, 13, 23, 33, and 43 min (C). (D) Time-dependent variations in the sizes of the mixture of apo-H-NHase (■) and holo-NhhAG (△). Apo-NHase (final concentration, 0.05 mg/mL), holo-NhhAG (final concentration, 0.5 mg/mL), and a mixture of apo-NHase and holo-NhhAG (final concentrations of 0.05 and 0.5 mg/mL, respectively) in 10 mM KPB (pH 7.5) were used to determine their sizes by DLS.

not involved in the simulation, being ascribed to the inhomogeneity of coordination with respect to the *z*-axis. On the other hand, such a spectrum was not observed for holo-NhhAG (Figure 5D). These findings revealed that there is a subtle difference in the coordination environments of the cobalt ions between holo-H-NHase and holo-NhhAG.

Metallochaperone NhhG. Cobalt is directly inserted into the apo α-subunit of apo-NhlAE in the presence of a reducing agent [dithiothreitol, 2-mercaptoethanol, or glutathione (GSH)]

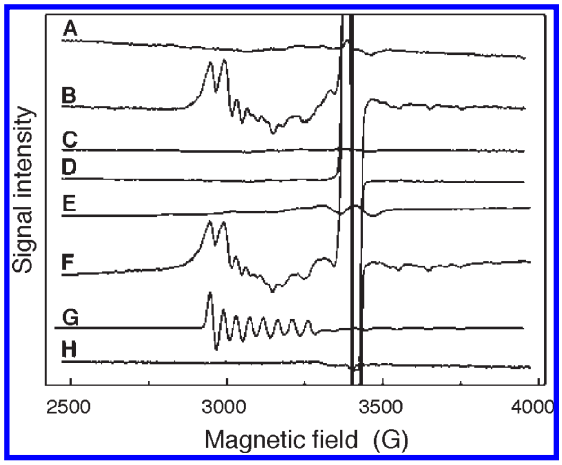

FIGURE 5: EPR spectra of holo-H-NHase, holo-NhhAG, and R-H-NHase. (A) Native holo-H-NHase. (B) Reduced holo-H-NHase with methyl viologen and sodium dithionite. (C) Native holo-NhhAG. (D) Reduced holo-NhhAG with methyl viologen and sodium dithionite. (E) Native R-H-NHase. (F) Reduced R-H-NHase with methyl viologen and sodium dithionite. (G) Simulation spectrum of spectra B and F. (H) Co^{2+} solution. A line width of 27 G was used for the simulation. The sharp feature at 3370 G is due to the reduced methyl viologen radical. Proteins (final concentration, 5 mg/mL) in 10 mM KPB (pH 7.5) and $CoCl_2$ (final concentration, 0.1 mM) in 10 mM KPB (pH 7.5) were used for EPR spectroscopy.

in vitro, suggesting that NhlE is also a metallochaperone that is crucial for the insertion of cobalt into the α-subunit of L-NHase (*35*). To elucidate the role of NhhG in the incorporation of cobalt into the α-subunit of H-NHase, we purified cobalt-free NhhAG (apo-NhhAG) expressed from pHJK19 (from a culture in the absence of cobalt) (Table 3). Although holo-NhhAG gave a band at 346 nm in the near-UV−vis CD spectrum, apo-NhhAG gave no such band (Figure 2E). Apo-NhhAG (final concentration, 0.1 mg/mL) was mixed with cobalt (final concentration, 20 μM) and GSH (1 mM) in 10 mM KPB (pH 7.5), followed by incubation at 28 °C. The reconstituted NhhAG (R-NhhAG) was purified after incubation for 2 h and then compared with holo-NhhAG and apo-NhhAG. The results of cobalt content determination showed that R-NhhAG contained 0.81 ± 0.03 mol of ion/mol of αg_2 (Table 3), which is similar to the content (0.84 ± 0.04 mol of ion/mol of αg_2) of holo-NhhAG (Table 1). Although R-NhhAG, holo-NhhAG, and apo-NhhAG exhibited similar far-UV CD spectra (Figure 2D), the UV−vis spectrum of R-NhhAG was similar to that of holo-NhhAG, but not to that of apo-NhhAG (Figure 2F). As shown in Figure 2F, an extra shoulder in the 300−350 nm region was found for R-NhhAG as well as holo-NhhAG.

R-NhhAG was also able to convert apo-H-NHase into holo-H-NHase (data not shown). These findings suggest that cobalt was directly incorporated into apo-NhhAG, resulting in the formation of holo-NhhAG. On the other hand, we also mixed apo-H-NHase with cobalt and GSH, purified the resultant apo-H-NHase (R-apo-H-NHase) after incubation for 2 h, and then compared it with holo-H-NHase and apo-H-NHase. The UV−vis spectrum of R-apo-H-NHase was similar to that of apo-H-NHase, but not to that of holo-H-NHase, and no extra shoulder in the 300−350 nm region was observed (Figure 2C). In contrast to the cobalt content of holo-H-NHase (0.90 ± 0.04 mol/mol of $\alpha\beta$), only 0.18 ± 0.02 mol of cobalt ion/mol of $\alpha\beta$ was detected in R-apo-H-NHase (Table 3). These findings demonstrate that a cobalt ion was directly incorporated into the apo α-subunit of apo-NhhAG, but not into that of apo-H-NHase in vitro, and that NhhG is involved in cobalt incorporation as a metallochaperone.

Table 3: Characterization of Purified Apo-NhhAG, Apo-H-NHase, and Purified Resultant (R-)NhhAG, and R-Apo-H-NHase after Being Mixed with Cobalt and GSH in Vitro[a]

protein	cobalt content (mol of ions/mol of protein)	specific activity (units/mg)
apo-NhhAG	$0.02 \pm 0.01/\alpha g_2$	0
R-NhhAG	$0.81 \pm 0.03/\alpha g_2$	0
apo-H-NHase	$0.04 \pm 0.01/\alpha\beta$	2.4 ± 0.5
R-apo-H-NHase	$0.18 \pm 0.02/\alpha g_2$	11.3 ± 0.3

[a]Values represent the means ± the standard deviation for at least three independent experiments.

Table 4: Strict Recognition of a NHase Mediator for Apo-NHase[a]

protein	cobalt content (mol of ions/mol of protein)	specific activity (units/mg)	N-terminal sequence of the α-subunit
apo-H-NHase	$0.04 \pm 0.01/\alpha\beta$	2.4 ± 0.5	^{2}SEH**V**NKY^8
holo-NhlAE	$0.85 \pm 0.03/\alpha e_2$	0	^{2}**T**AHNP^6
R-apo-H-NHase$_{(NhlAE)}$	$0.05 \pm 0.01/\alpha\beta$	2.1 ± 0.6	^{2}SEH**V**NKY^8
apo-L-NHase	$0.02 \pm 0.01/\alpha\beta$	4.2 ± 0.8	^{2}**T**AHNP^6
holo-NhhAG	$0.84 \pm 0.04/\alpha g_2$	0	^{2}SEH**V**NKY^8
R-apo-L-NHase$_{(NhhAG)}$	$0.04 \pm 0.01/\alpha\beta$	5.1 ± 0.4	^{2}**T**AHNP^6

[a]The third N-terminal amino acid of each L-NHase α-subunit and the fifth one of each H-NHase α-subunit are shown in bold. Values represent the means ± the standard deviation for at least three independent experiments.

Strict Recognition of a NHase Mediator for Apo-NHase. We here discovered a second NHase mediator (Table 1) and that the self-subunit swapping process is involved in both L-NHase (*30*) and H-NHase formation. Because the α-subunit of H-NHase is significantly similar in sequence to that of L-NHase (*45*), we investigated whether α-subunit exchange occurs between apo-H-NHase and a L-NHase mediator (holo-NhlAE) or between apo-L-NHase and a H-NHase mediator (holo-NhhAG). The purified apo-H-NHase (final concentration, 0.01 mg/mL) was mixed with the purified holo-NhlAE (final concentration, 0.1 mg/mL), followed by incubation in 10 mM KPB (pH 7.5) at 28 °C, and then the resultant H-NHase [R-apo-H-NHase$_{(NhlAE)}$] was purified from the mixture after incubation for 16 h. The R-apo-H-NHase$_{(NhlAE)}$ retained low H-NHase activity and a low cobalt content like apo-H-NHase (Table 4). On N-terminal amino acid sequence analysis of the α-subunit of the purified R-apo-H-NHase$_{(NhlAE)}$, the α-subunit of apo-H-NHase was found to remain in the R-apo-H-NHase$_{(NhlAE)}$, demonstrating that the apo α-subunit of apo-H-NHase was not replaced by the holo α-subunit of holo-NhlAE. Similarly, the purified apo-L-NHase (final concentration, 0.01 mg/mL) was mixed with the purified holo-NhhAG (final concentration, 0.1 mg/mL), followed by incubation in 10 mM KPB (pH 7.5) at 28 °C, and then the resultant L-NHase [R-apo-L-NHase$_{(NhhAG)}$] was purified from the mixture after incubation for 16 h. As a result, we found that R-apo-L-NHase$_{(NhhAG)}$ also exhibited low L-NHase activity and no increase in cobalt content and included the α-subunit of apo-L-NHase (Table 4), demonstrating that the apo α-subunit of apo-L-NHase was not replaced by the holo α-subunit of holo-NhhAG.

DISCUSSION

The incorporation of cobalt into L-NHase consisting of a heterotetramer ($\alpha_2\beta_2$) (approximately 100 kDa) has been found to depend on the α-subunit exchange (self-subunit swapping) between apo-L-NHase and its cobalt-containing mediator, holo-NhlAE, NhlE having been recognized as a self-subunit swapping chaperone (*30*). We here confirmed that H-NHase also post-translationally matures through self-subunit swapping. The occurrence of self-subunit swapping maturation even in the large enzyme H-NHase consisting of a multimer of $\alpha\beta$ heterodimers (approximately 500 kDa) is very surprising and very interesting. On the basis of the features shared by L-NHase, H-NHase, and other various Co-NHases described above (Table S2 of the Supporting Information), these findings strongly suggest that self-subunit swapping occurs not only in L-NHase and H-NHase but also in the Co-NHases and that the small proteins whose genes are located just downstream of the NHase α-subunit genes are self-subunit swapping chaperones. In addition, self-subunit swapping might also occur in SCNase [which has a heterododecameric structure, $(\alpha\beta\gamma)_4$] (*26*, *27*). P15K, which is essential for functional expression of SCNase, is reported to have an amino acid sequence similar to that of NhlE, NhhG, and P14K in *B. pallidus* RAPc8 (*40*). Like the genes for the self-subunit swapping chaperones of L-NHase and H-NHase, that for P15K is located just downstream of the gene for a metal-containing subunit, the γ-subunit (corresponding to the NHase α-subunit) (Figure S3 of the Supporting Information). SCNase expressed in the absence of P15K is an apoenzyme (*26*), suggesting that P15K is likely to promote the functional expression of SCNase in vivo by assisting the incorporation of a metal ion. Moreover, P15K forms a complex with the cobalt-containing subunit (γ-subunit) of SCNase, supporting the possibility that the functional expression of SCNase depends on self-subunit swapping. Together with these results, our findings show that self-subunit swapping is one of the general maturation mechanisms for multisubunit metalloenzymes.

All α-subunits of the reported NHases share a characteristic metal-binding motif [CXLC(SO_2H)SC(SOH)] containing two modified cysteine residues (*4*, *20*−*24*). Metal ion binding is responsible for the post-translational modification of the two cysteines in the α-subunit of NHase (*1*, *29*, *30*), but such modification has not been observed in apo-NHase (*25*). The post-translationally modified Cys-SO_2H and Cys-SOH in NHase have deprotonated Cys-SO_2^- and Cys-SO^- structures, respectively (*3*), and the deprotonated Cys-SO_2^- and Cys-SO^- in the holo α-subunit form salt bridges with the two arginines of the β-subunit (which are conserved in all known Co-type and Fe-type NHases) in the holoenzyme (*20*−*23*). It has been demonstrated that the modified cysteines exist in the L-NHase mediator holo-NhlAE and that the electrostatic interaction needed to form the salt bridge between the two negatively charged modified cysteines (Cys112-SO_2^- and Cys114-SO^-) of the α-subunit in holo-NhlAE and the two positively charged arginines (R52 and R157) of the β-subunit in apo-L-NHase provides the driving force for α-subunit exchange (*30*). Considering these findings, we can easily expect that the two corresponding cysteines (αCys105 and αCys107) are modified in holo-H-NHase and holo-NhhAG, but not in apo-H-NHase or apo-NhhAG, and that the electrostatic interaction needed to form the salt bridges between the two negatively charged modified cysteines (αCys105-SO_2^- and αCys107-SO^-) in holo-NhhAG and the two corresponding positively charged arginines (R52 and R160) of the β-subunit in apo-H-NHase provides the driving force for α-subunit exchange during H-NHase maturation.

Self-subunit swapping chaperones (NhhG and NhlE) and the putative self-subunit swapping chaperones (P14K, P15K, etc.) do not exhibit significant sequence similarity with known

metallochaperones (containing the CXCC metal-binding motif) involved in the maturation of Fe-NHases. The genes encoding the metallochaperones for Fe-type NHases are located just downstream of the genes encoding the β-subunits of Fe-type NHases, whereas the genes encoding the self-subunit swapping chaperones are located just downstream of the genes encoding the α-subunits of Co-type NHases. The calculated molecular mass for each of the activators for Fe-type NHases (~50 kDa) differs from those of the self-subunit swapping chaperones (< 17 kDa). These findings indicate that the mechanisms of post-translational activation are quite different between Co-type NHases (including related cobalt-containing enzyme SCNase) and Fe-type NHases: NhlE, NhhG, P14K, P15K, etc., act as self-subunit swapping chaperones, in contrast with the activators that act as metallochaperones for Fe-type NHases.

Though the α-subunits of H-NHase and L-NHase exhibit significant sequence similarity (53% identical), NhlE is able to form a complex with the α-subunit of L-NHase, but probably not with that of H-NHase (Figure S5 of the Supporting Information). These findings suggest that NhlE recognizes only NhlA, i.e., not NhhA. Moreover, α-subunit exchange occurs between holo-NhlAE and apo-L-NHase (*30*), but not between holo-NhlAE and apo-H-NHase (Table 4). These phenomena may be due to the precise recognition by the self-subunit swapping charperone of its specific α-subunit. We demonstrated that both NhlAE and NhhAG consist of heterotrimers (αe_2 and αg_2), and the resultant NhlE isolated from NhlAE through denaturation and renaturation exhibits a dimeric assembled form (e_2) (*30*). These findings suggested that the structures of αe_2 and αg_2 would be α-e_2 (not e-α-e) and α-g_2 (not g-α-g), respectively. Considering these findings, we propose a possible model for self-subunit swapping in L-NHase, instead of H-NHase, for an improved understanding (Figure 6): one e protein has one binding site for the α-subunit (NhlA) of L-NHase, and thus one e_2 carries two binding sites for the α-subunit (NhlA) of L-NHase; one of the binding sites is occupied by the holo α-subunit (NhlA) of holo-αe_2, and the other is free; after the addition of apo-L-NHase to holo-NhlAE, the apo α-subunit in apo-L-NHase approaches and binds to the other empty recognition (binding) site of e_2, and then the β-subunit (of apo-L-NHase) and the holo α-subunit (of holo-NhlAE) begin to be attracted through the electrostatic interaction and then associate with each other. Sequentially, the apo α-subunit of apo-L-NHase is extruded by the holo α-subunit of NhlAE, resulting in the formation of holo-L-NHase. Self-subunit swapping in H-NHase should be the same as that in L-NHase. As a result of DLS analyses, we, for the first time, detected intermediate complexes consisting of apo-H-NHase and holo-NhhAG during self-subunit swapping. The largest intermediate was ~2 times larger than holo-H-NHase in hydrodynamic diameter. The discovery of intermediate complexes larger in size than H-NHase strongly supports the above-mentioned possible model for self-subunit swapping. One of the apo α-subunits in apo-H-NHase would associate with the holo α-subunit of holo-αg_2 via the two binding sites for the α-subunit of a dimeric assembled form (g_2) in the intermediate complexes. On the basis of time-dependent variations in the sizes of the mixture of apo-H-NHase and holo-αg_2 (Figure 4C,D), this recognition and binding to form various intermediate complexes occur rapidly (within 3 min). In a mixture of holo-αg_2 and apo-L-NHase, however, one of the apo α-subunits of apo-L-NHase did not bind to the empty binding site of g_2 in holo-αg_2, because NhhG recognized only the α-subunit (NhhA) of H-NHase,

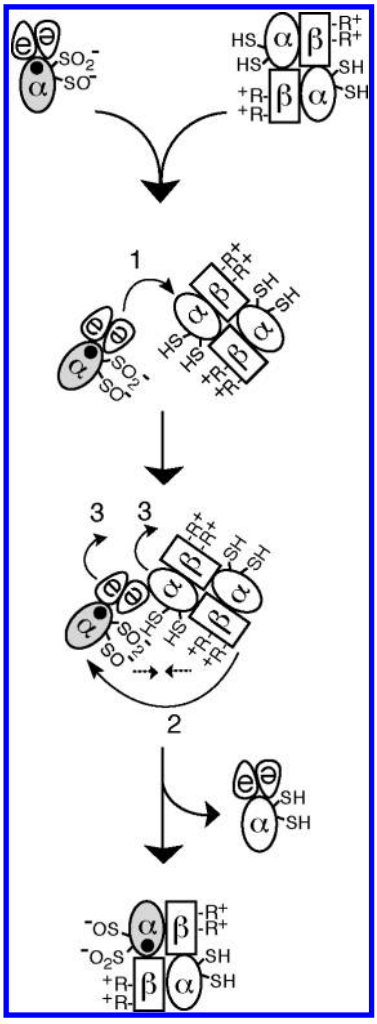

FIGURE 6: Proposed mechanism for self-subunit swapping. Step 1 involves access of the apo α-subunit to e_2. Step 2 is association between the β-subunit and the holo α-subunit. Step 3 consists of dissociation and association of the α-subunit and e_2. The two cysteines in the apo α-subunit are denoted as -SH, and the two modified cysteines in the holo α-subunit are denoted as $-SO^-$ and $-SO_2^-$, respectively. The two arginines in the β-subunit are denoted as $-R^+$. The dotted line with the arrow shows the electrostatic attraction between the two modified cysteines and the two arginines.

i.e., not that (NhlA) of L-NHase, and α-subunit exchange therefore did not occur between apo-L-NHase and holo-NhhAG. Similarly, NhlE recognized only the α-subunit of L-NHase, i.e., not that of H-NHase, and thus, α-subunit exchange did not occur between apo-H-NHase and holo-NhlAE. These findings reveal that self-subunit swapping is a α-subunit-specific reaction.

NhlAE is a vital complex for the incorporation of cobalt into the α-subunit of L-NHase, and NhlE has been shown to facilitate Cys-SOH and Cys-SO_2H modification in the α-subunit of L-NHase post-translationally (*35*). Considering these findings, we propose that a self-subunit swapping chaperone also functions as a metallochaperone, which also has a redox function. Each of the self-subunit swapping chaperone genes is located just downstream of the corresponding α-subunit gene (or the γ-subunit gene of SCNase) (Figure S3 of the Supporting Information), and exhibits significant sequence similarity to the corresponding β-subunit gene. Why the $\beta-\alpha-$(self-subunit swapping chaperone) gene order exists for Co-type NHase and why the $\alpha-\beta-$(metallochaperone) gene order exists for Fe-type NHase remained unknown for a long time (Figure S3 of the Supporting Information).

The existence of both NhlAE and NhhAG suggested that the $\beta-\alpha-$(self-subunit swapping chaperone) gene order allows each of the self-subunit swapping chaperones to easily associate with the corresponding apo α-subunit after translation, resulting in the formation of the corresponding NHase mediator (NhhAG, NhlAE, etc.), which is crucial for cobalt insertion and cysteine modification post-translationally. From the transformant harboring a plasmid, pHJK19$_{(\Delta G)}$ (Figure S2 of the Supporting Information), we purified H-NHase$_{(\Delta G)}$ with low activity [only 2% of that of H-NHase$_{(+G)}$] containing a small amount of cobalt [0.33 mol/mol of $\alpha\beta$, i.e., ~30% of that in H-NHase$_{(+G)}$] in this study (Table 1). In both the near-UV−vis CD and UV−vis spectra of H-NHase$_{(\Delta G)}$, no extra shoulder in the 300−350 nm region was observed, suggesting that the Co ligand environment of H-NHase$_{(\Delta G)}$ is different from that of H-NHase$_{(+G)}$. These findings indicate that the active center of H-NHase$_{(\Delta G)}$ was not constructed correctly without the participation of *nhhG*, although a small amount of cobalt was incorporated into H-NHase. Therefore, we here clarify that, during the biogenesis of these enzymes, the metal should be first inserted into the apo α-subunit of the mediator complex (NhhAG, NhlAE, etc.) with the participation of the self-subunit swapping chaperone as a metallochaperone and then incorporated into NHase (or SCNase) through self-subunit swapping maturation.

We expected that the cobalt ion in holo-NhhAG would be a low-spin Co^{3+} for the following reasons. (i) The low-spin Co^{3+}-containing α-subunit of holo-H-NHase was derived from holo-NhhAG. (ii) The absorption in the 300−350 nm region reflecting S → Co^{3+} charge transfer was observed in the UV spectrum of holo-NhhAG (Figure 2F). (iii) Holo-NhhAG gave a band at 346 nm in the near-UV−vis CD spectrum reflecting S → Co^{3+} charge transfer (Figure 2E). (iv) The incorporation of cobalt into the L-NHase mediator (NhlAE) was associated with the oxidation of Co^{2+} to Co^{3+} (*35*). However, an EPR spectrum characteristic of low-spin Co^{2+} observed for reduced holo-H-NHase was not observed for reduced holo-NhhAG. The results of EPR analysis suggested that there is a subtle difference in the coordination environments of the cobalt ions between holo-H-NHase and holo-NhhAG. Because the change in the redox potential of the cobalt ion was due to the subtle difference between them, the Co^{3+} in holo-NhhAG could not be reduced even under the reduced conditions used for holo-H-NHase. Inferential support for the subtle differences is also provided by comparison of the near-UV−vis CD spectra of holo-H-NHase and holo-NhhAG. The peaks at 405 and 444 nm in the near-UV−vis CD spectrum of holo-H-NHase were not seen in that of holo-NhhAG. The subtle differences in the coordination environments of the cobalt ions between H-NHase and NhhAG are also supported by the different colors observed for holo-H-NHase and holo-NhhAG; the concentrated holo-H-NHase was pink in color, while the concentrated holo-NhhAG was orange in color. These findings suggest that self-subunit swapping maturation includes not only the exchange of two α-subunits but also the alteration of the cobalt coordination environment.

Self-subunit swapping is one of the means of post-translational maturation for incorporation of metal ion into target multisubunit metalloproteins. It may also occur during the activation (modification) of enzymes with various types of cofactor(s) (e.g., metal ions, iron−sulfur clusters, and coenzymes) and raises the possibility that similar behavior of a protein, namely "self-component swapping", occurs in other forms of post-translational activation, post-translational modification, and allosteric conformational changes of protein complexes.

ACKNOWLEDGMENT

We thank Dr. T. Sakashita for amino acid sequence analysis. We also thank Dr. K. Shiraki for CD spectral analysis, Prof. Y. Nagasaki for DLS analysis, and Prof. K. Fujisawa for the helpful discussion.

SUPPORTING INFORMATION AVAILABLE

Specific recognition of a self-subunit swapping chaperone for the α-subunit (Supporting Results), primers used in this study (Table S1), Co-NHase-related small proteins showing significant sequence similarity to NhlE (Table S2), self-subunit swapping maturation (Figure S1), genetic organization for the construction of the set of plasmids used in this study (Figure S2), schematic representation of L-NHase, other Co- and Fe-NHases, and SCNase (Figure S3), dynamic light scattering analyses of holo-H-NHase and apo-NhhAG (Figure S4), and SDS−PAGE of a cell-free extract of each *R. fascians* DSM43985 transformant (Figure S5). This material is available free of charge via the Internet at http://pubs.acs.org.

REFERENCES

1. Kobayashi, M., and Shimizu, S. (1998) Metalloenzyme nitrile hydratase: Structure, regulation, and application to biotechnology. *Nat. Biotechnol. 16*, 733–736.
2. Asano, Y., Tani, Y., and Yamada, H. (1980) A new enzyme "nitrile hydratase" which degrades acetonitrile in combination with amidase. *Agric. Biol. Chem. 44*, 2251–2252.
3. Noguchi, T., Nojiri, M., Takei, K., Odaka, M., and Kamiya, N. (2003) Protonation structures of Cys-sulfinic and Cys-sulfenic acids in the photosensitive nitrile hydratase revealed by Fourier transform infrared spectroscopy. *Biochemistry 42*, 11642–11650.
4. Greene, S. N., and Richards, N. G. (2006) Electronic structure, bonding, spectroscopy and energetics of Fe-dependent nitrile hydratase active-site models. *Inorg. Chem. 45*, 17–36.
5. Komeda, H., Kobayashi, M., and Shimizu, S. (1996) A novel gene cluster including the *Rhodococcus rhodochrous* J1 *nhlBA* genes encoding a low molecular mass nitrile hydratase (L-NHase) induced by its reaction product. *J. Biol. Chem. 271*, 15796–15802.
6. Kobayashi, M., and Shimizu, S. (1999) Cobalt proteins. *Eur. J. Biochem. 261*, 1–9.
7. Payne, M. S., Wu, S., Fallon, R. D., Tudor, G., Stieglitz, B., Turner, I. M., Jr., and Nelson, M. J. (1997) A stereoselective cobalt-containing nitrile hydratase. *Biochemistry 36*, 5447–5454.
8. Kobayashi, M., Fujiwara, Y., Goda, M., Komeda, H., and Shimizu, S. (1997) Identification of active sites in amidase: Evolutionary relationship between amide bond- and peptide bond-cleaving enzymes. *Proc. Natl. Acad. Sci. U.S.A. 94*, 11986–11991.
9. Hashimoto, Y., Hosaka, H., Oinuma, K., Goda, M., Higashibata, H., and Kobayashi, M. (2005) Nitrile pathway involving acyl-CoA synthetase: Overall metabolic gene organization and purification and characterization of the enzyme. *J. Biol. Chem. 208*, 8660–8667.
10. Abe, T., Hashimoto, Y., Hosaka, H., Tomita-Yokotani, K., and Kobayashi, M. (2008) Discovery of amide (peptide) bond synthetic activity in acyl-CoA synthetase. *J. Biol. Chem. 283*, 11312–11321.
11. Komeda, H., Hori, Y., Kobayashi, M., and Shimizu, S. (1996) Characterization of the gene cluster of high-molecular-mass nitrile hydratase (H-NHase) induced by its reaction product in *Rhodococcus rhodochrous* J1. *Proc. Natl. Acad. Sci. U.S.A. 93*, 10572–10577.
12. Komeda, H., Kobayashi, M., and Shimizu, S. (1997) A novel transporter involved in cobalt uptake. *Proc. Natl. Acad. Sci. U.S.A. 94*, 36–41.
13. Komeda, H., Kobayashi, M., and Shimizu, S. (1996) Characterization of the gene cluster of high-molecular-mass nitrile hydratase (H-NHase) induced by its reaction product in *Rhodococcus rhodochrous* J1. *Proc. Natl. Acad. Sci. U.S.A. 93*, 4267–4272.
14. Kobayashi, M., Nagasawa, T., and Yamada, H. (1992) Enzymatic synthesis of acrylamide: A success story not yet over. *Trends Biotechnol. 10*, 402–408.
15. Zhou, Z., Hashimoto, Y., and Kobayashi, M. (2005) Nitrile degradation by *Rhodococcus*: Useful microbial metabolism for industrial productions. *Actinomycetologica 19*, 18–26.
16. Mitra, S., Job, K. M., Meng, L., Bennett, B., and Holz, R. C. (2008) Analyzing the catalytic role of Asp97 in the methionine aminopeptidase from *Escherichia coli*. *FEBS J. 275*, 6248–6259.

17. Cai, J., Han, C., Hu, T., Zhang, J., Wu, D., Wang, F., Liu, Y., Ding, J., Chen, K., Yue, J., Shen, X., and Jiang, H. (2006) Peptide deformylase is a potential target for anti-*Helicobacter pylori* drugs: Reverse docking, enzymatic assay, and X-ray crystallography validation. *Protein Sci. 15*, 2071–2081.
18. Chae, P. S., Kim, M. S., Jeung, C. S., Lee, S. D., Park, H., Lee, S., and Suh, J. (2005) Peptide-cleaving catalyst selective for peptide deformylase. *J. Am. Chem. Soc. 127*, 2396–2397.
19. Deng, H., Callender, R., Zhu, J., Nguyen, K. T., and Pei, D. (2002) Determination of the ionization state and catalytic function of Glu-133 in peptide deformylase by difference FTIR spectroscopy. *Biochemistry 41*, 10563–10569.
20. Hourai, S., Miki, M., Takashima, Y., Mitsuda, S., and Yanagi, K. (2003) Crystal structure of nitrile hydratase from a thermophilic *Bacillus smithii*. *Biochem. Biophys. Res. Commun. 312*, 340–345.
21. Miyanaga, A., Fushinobu, S., Ito, K., and Wakagi, T. (2001) Crystal structure of cobalt-containing nitrile hydratase. *Biochem. Biophys. Res. Commun. 288*, 1169–1174.
22. Nagashima, S., Nakasako, M., Dohmae, N., Tsujimura, M., Takio, K., Odaka, M., Yohda, M., Kamiya, N., and Endo, I. (1998) Novel non-heme iron center of nitrile hydratase with a claw setting of oxygen atoms. *Nat. Struct. Biol. 5*, 347–351.
23. Huang, W., Jia, J., Cummings, J., Nelson, M., Schneider, G., and Lindqvist, Y. (1997) Crystal structure of nitrile hydratase reveals a novel iron centre in a novel fold. *Structure 5*, 691–699.
24. Stevens, J. M., Belghazi, M., Jaouen, M., Bonnet, D., Schmitter, J. M., Mansuy, D., Sari, M. A., and Artaud, I. (2003) Post-translational modification of *Rhodococcus* R312 and *Comamonas* NI1 nitrile hydratases. *J. Mass Spectrom. 38*, 955–961.
25. Miyanaga, A., Fushinobu, S., Ito, K., Shoun, H., and Wakagi, T. (2004) Mutational and structural analysis of cobalt-containing nitrile hydratase on substrate and metal binding. *Eur. J. Biochem. 271*, 429–438.
26. Kataoka, S., Arakawa, T., Hori, S., Katayama, Y., Hara, Y., Matsushita, Y., Nakayama, H., Yohda, M., Nyunoya, H., Dohmae, N., Maeda, M., and Odaka, M. (2006) Functional expression of thiocyanate hydrolase is promoted by its activator protein, P15K. *FEBS Lett. 580*, 4667–4672.
27. Arakawa, T., Kawano, Y., Kataoka, S., Katayama, Y., Kamiya, N., Yohda, M., and Odaka, M. (2007) Structure of thiocyanate hydrolase: A new nitrile hydratase family protein with a novel five-coordinate cobalt(III) center. *J. Mol. Biol. 366*, 1497–1509.
28. Katayama, Y., Hashimoto, K., Nakayama, H., Mino, H., Nojiri, M., Ono, T. A., Nyunoya, H., Yohda, M., Takio, K., and Odaka, M. (2006) Thiocyanate hydrolase is a cobalt-containing metalloenzyme with a cysteine-sulfinic acid ligand. *J. Am. Chem. Soc. 128*, 728–729.
29. Kuchar, J., and Hausinger, R. P. (2004) Biosynthesis of metal sites. *Chem. Rev. 104*, 509–525.
30. Zhou, Z., Hashimoto, Y., Shiraki, K., and Kobayashi, M. (2008) Discovery of posttranslational maturation by self-subunit swapping. *Proc. Natl. Acad. Sci. U.S.A. 105*, 14849–14854.
31. Lu, J., Zheng, Y., Yamagishi, H., Odaka, M., Tsujimura, M., Maeda, M., and Indo, I. (2003) Motif CXCC in nitrile hydratase activator is critical for NHase biogenesis *in vivo*. *FEBS Lett. 553*, 391–396.
32. Nojiri, M., Yohda, M., Odaka, M., Matsushita, Y., Tsujimura, M., Yoshida, T., Dohmae, N., Takio, K., and Endo, I. (1999) Functional expression of nitrile hydratase in *Escherichia coli*: Requirement of a nitrile hydratase activator and post-translational modification of a ligand cysteine. *J. Biochem. 125*, 696–704.
33. Wu, S., Fallon, R., and Payne, M. (1997) Over-production of stereoselective nitrile hydratase from *Pseudomonas putida* 5B in *Escherichia coli*: Activity requires a novel downstream protein. *Appl. Microbiol. Biotechnol. 48*, 704–708.
34. Hashimoto, Y., Nishiyama, M., Horinouchi, S., and Beppu, T. (1994) Nitrile hydratase gene from *Rhodococcus sp.* N-774 requirement for its downstream region for efficient expression. *Biosci., Biotechnol., Biochem. 58*, 1859–1865.
35. Zhou, Z., Hashimoto, Y., and Kobayashi, M. (2009) Self-subunit swapping chaperone needed for the maturation of multimeric metalloenzyme nitrile hydratase by a subunit exchange mechanism also carries out the oxidation of the metal ligand cysteine residues and insertion of cobalt. *J. Biol. Chem. 284*, 14930–14938.
36. Cunningham, F. X., Jr., and Gantt, E. (2001) One ring or two? Determination of ring number in carotenoids by lycopene ε-cyclases. *Proc. Natl. Acad. Sci. U.S.A. 98*, 2905–2910.
37. Pogulis, R. J., Yallejo, A. N., and Pease, L. R. (1996) *In vitro* recombination and mutagenesis by overlap extension PCR. *Methods Mol. Biol. 57*, 167–176.
38. Hashimoto, Y., Nishiyama, M., Yu, F., Watanabe, I., Horinouchi, S., and Beppu, T. (1992) Development of a host-vector system in a *Rhodococcus* strain and its use for expression of the cloned nitrile hydratase gene cluster. *J. Gen. Microbiol. 138*, 1003–1010.
39. Stoll, S., and Schweiger, A. (2006) EasySpin, a comprehensive software package for spectral simulation and analysis in EPR. *J. Magn. Reson. 178*, 42–55.
40. Cameron, R. A., Sayed, M., and Cowan, D. A. (2005) Molecular analysis of the nitrile catabolism operon of the thermophile *Bacillus pallidus* RAPc8. *Biochim. Biophys. Acta 1725*, 35–46.
41. Nagasawa, T., Takeuchi, K., and Yamada, H. (1991) Characterization of a new cobalt-containing nitrile hydratase purified from urea-induced cells of *Rhodococcus rhodochrous* J1. *Eur. J. Biochem. 196*, 581–589.
42. Nojiri, M., Nakayama, H., Odaka, M., Yohda, M., Takio, K., and Endo, I. (2000) Cobalt-substituted Fe-type nitrile hydratase of *Rhodococcus* sp. N-771. *FEBS Lett. 465*, 173–177.
43. Arakawa, T., Kawano, Y., Katayama, Y., Nakayama, H., Dohmae, N., Yohda, M., and Odaka, M. (2009) Structural basis for catalytic activation of thiocyanate hydrolase involving metal-ligated cysteine modification. *J. Am. Chem. Soc. 131*, 14838–14843.
44. Brennan, B. A., Alms, G., Nelson, M. J., Durney, L. T., and Scarrow, R. C. (1996) Nitrile hydratase from *Rhodococcus rhodochrous* J1 contains a non-corrin cobalt ion with two sulfur ligands. *J. Am. Chem. Soc. 118*, 9194–9195.
45. Kobayashi, M., Nishiyama, M., Nagasawa, T., Horinouchi, S., Beppu, T., and Yamada, H. (1991) Cloning, nucleotide sequence and expression in *Escherichia coli* of two cobalt-containing nitrile hydratase genes from *Rhodococcus rhodochrous* J1. *Biochim. Biophys. Acta 1129*, 23–33.